INFLUENCE OF Ti DOPING ON THE ELECTRICAL PROPERTIES OF Sr_2FeNiO_6 NANOCOMPOSITES

P. R. Padole, A. A. Jadhao, G. N. Chaudhari, H. G. Wankhade*

Nanotechnology Research Laboratory, Department of Chemistry, Shri Shivaji Science College, Amravati (M.S), India.

Abstract

We have investigated the effect of Ti doping on structural and electrical properties of double perovskite $Sr_2Fe_{1-x}Ti_xMn_{0.2}NiO_6$(x= 0, 0.2, 0.4, and 0.6) nanocomposites via Sol gel citrate method. The structure of the Ti doped double perovskite is tetragonal structure**.** Moreover, the compositional feature of $Sr_2Fe_{1-x}Ti_xMn_{0.2}NiO_6$ nanocomposites was investigated through energy dispersive X-ray spectroscopy (EDS) analysis.Impedance analysis shows the presence of mostly bulk resistive (grain) contributions which is found to decrease with the increase in Ti concentration. The electrical conductivities are enhanced with increasing Ti content due to the greater amount of electronic holes originating from the increased interstitial oxygen.

Key Word: Sol gel citrate; Double-Pervoskite; Nanocomposites; Electrical conductivity.

1. Introduction

Nowadays, many researchers are interested in double perovskite oxides that consist of transition metals [1]. These materials cover a large part of material science research because of thevarious alluring chemical and physical properties such as thermal, electrical, optical, magnetic and biological [2-8] and their diverse applications in the fields such as electronics, sensors, magnetic memory components, fuel cells, and solar cells [9-12].

The B-site ordered double-perovskite compounds with chemical formula of $A_2B'B''O_{6-\delta}$ are derived from the simple perovskite ABO_3 through arranging two different cations B′ and B″ on the B-site. In this formula A stands for alkaline earth metal ions (like Ba, Ca, Sr) and especially rare earth elements and B′, B″ are transition metal ions [14]. Ideally, the framework of double-perovskite structure form is constructed by corner-shared $B'O_6$ and $B''O_6$octahedra in the lattices [15].

The double-perovskite oxide compounds are synthesized at high temperatures and have a very high flexibility in crystal structure and chemical composition. Where it is possible to add or replace the A-sites and B-sites cations with the continuation of the octahedra network connection. Many of the physical properties of double perovskites depend crucially on the details of these distortions, particularly the electronic, magnetic and dielectric properties which are so important for many of the applications of double perovskites. Recently, perovskites have gained attention as ionic and mixed conductors for solid-oxide fuel cell (SOFC) applications as electrodes and electrolytes.

In the present research article, as-synthesized $Sr_2Fe_{1-x}Ti_xMn_{0.2}NiO_6$double perovskitenanocomposites by sol-gel citrate method have been reported. The surface morphological study of prepared sample was studied using field emission scanning electron microscopy (FE-SEM) and elemental compositional study was done using Energy Dispersive X-ray Spectroscopy (EDS). The purpose of present study is to investigate the effect of Ti dopant on the structural and electrical properties of$Sr_2Fe_{1-x}Ti_xMn_{0.2}NiO_6$. An extensive dielectric and impedance analysis of $Sr_2Fe_{1-x}Ti_xMn_{0.2}NiO_6$(x= 0.2, 0.4, 0.6 and 0.8) nanocomposites has been performed in the temperature range of Room temp to 700°C within the frequency domain of 42 Hz to 500 KHz.

2. Experimental

2.1 Materials and methods

Double perovskite$Sr_2Fe_{1-x}Ti_xMn_{0.2}NiO_6$(x=0.2, 0.4, 0.6 and 0.8) nanocomposites were prepared by using sol-gel citrate method. The stoichiometric mixtures of Strontium nitrate [$Sr(NO_3)_2$], Ferric nitrate[$Fe(NO_3)_3.9H_2O$], Nickel Nitrate[$Ni(NO_3)_2.6H_2O$],Titanium Nitrate[$Ti(NO_3)_4$] and Manganese Nitrate[$Mn(NO_3)_2.4H_2O$] were of AR-grade and procured from SD Fine chemicals, India.Given stoichiometric mixtures magnetically stirred with citric acid as a chelating agent and ethanol at 80°C for 3hrs to get homogeneous solution. The solution was further heated at about 130° for 12 hrs in pressure vessel to get gel precursor. Then it was subjected to 3hrs heat treatment at 350°C in muffle furnace. After heat treatment it milled to a fine powder. The dried powder sample was calcinated in range of 350°- 650°C in order to improve the crystalinity of material.

2.2 Characterization

The structure and crystallite size of $Sr_2Fe_{1-x}Ti_xMn_{0.2}NiO_6$(x= 0, 0.2, 0.4 and 0.6) nanocomposites have been investigated using Rigaku X-ray diffractometer with Cu Kα radiation .Samples were scanned through an angle of 20°–70° at a scanning speed of 2 .9 $x10^{-4}$ rad/s. Surface morphology of prepared nanocomposites has been investigated using Field emission scanning electron microscopy (FE-SEM) (S-4800, Hitachi, Japan). The composition was determined with Energy Dispersive X-ray Spectroscopy (EDS) attached with FE-SEM (Brucker, Japan).Using LCR HI-Tester (HIOKI 3532-50).

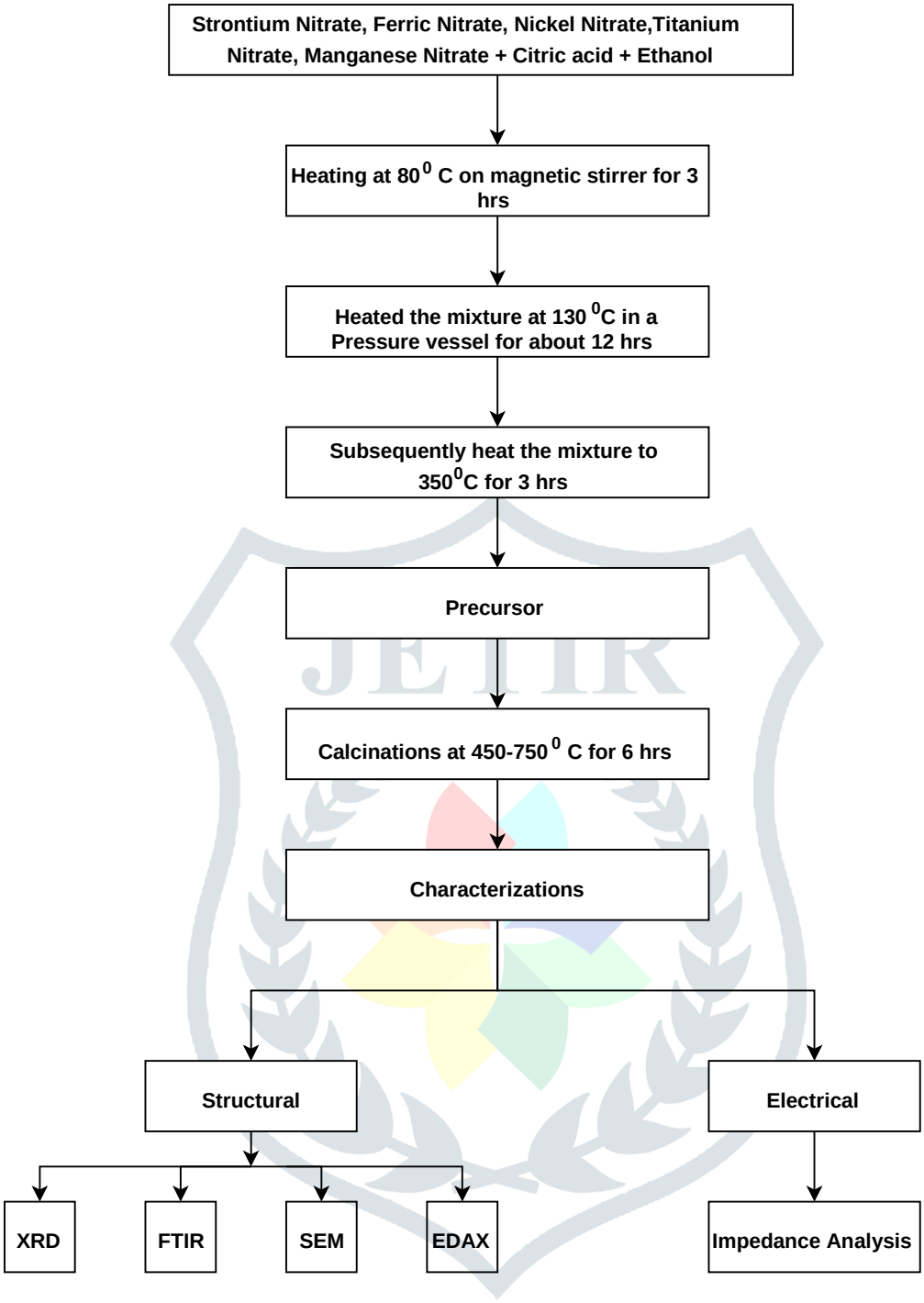

Fig. 1 Flow chart for the preparation of $Sr_2Fe_{1-x}Ti_xMn_{0.2}NiO_6$ double perovskite nanocomposites.

3. Results and Discussions

3.1. Structural analysis

3.1.1. X-ray diffraction

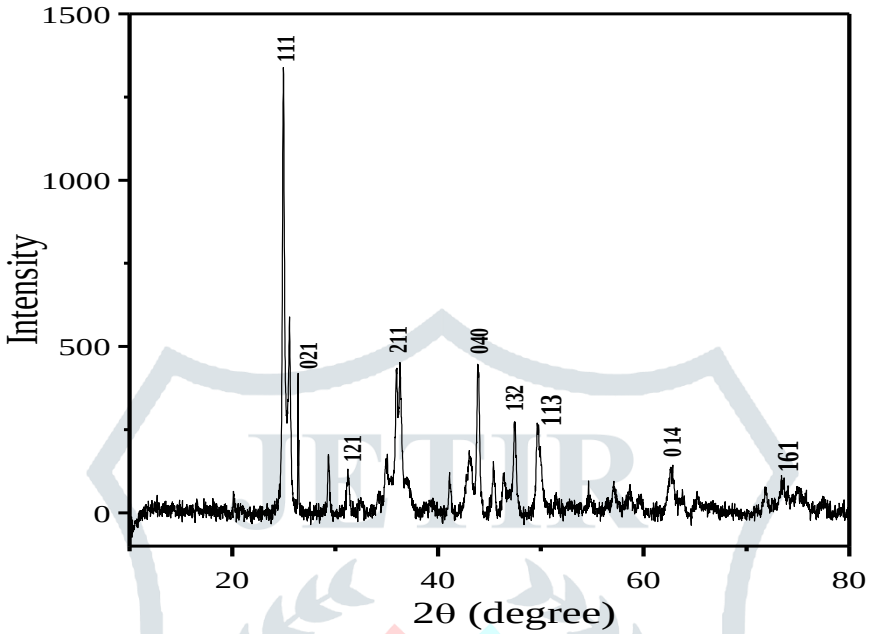

Fig. 2 X-ray diffraction pattern of the synthesized $Sr_2Fe_{1-x}Ti_xMn_{0.2}NiO_6$calcined at 650^0C.

The structure and crystallite size of $Sr_2Fe_{1-x}Ti_xMn_{0.2}NiO_6$nanocomposites was conformed with the help of XRD. Fig.2 shows the XRD pattern of $Sr_2Fe_{1-x}Ti_xMn_{0.2}NiO_6$nanocomposites prepared by sol–gel citrate exhibit typical reflections from (1 1 1), (02 1), (1 2 1), (2 1 1), (0 4 0) and (1 3 2) planes which indicate the presence of tetragonal structure. These diffraction lines confirm the formation of $Sr_2Fe_{1-x}Ti_xMn_{0.2}NiO_6$. The crystallite size of $Sr_2Fe_{1-x}Ti_xMn_{0.2}NiO_6$nanocomposites was calculated using the Scherrer's relation [12].

$$= D\frac{k\lambda}{\beta cos\theta} \qquad (1)$$

Where D is the crystallite size, k = 0.9 is a correction factor to account for particle shapes, is the full width at half maximum (FWHM) of the peaks of all planes in the XRD pattern, λ is the wavelength of Cu target = 1.5406 A˚, and θ is the Bragg angle

The distribution of the average crystallite size nanocomposites synthesized through sol–gel methods was found to be ~18.1 nm.

3.1.2. Scanning electron microscopy (SEM) Analysis

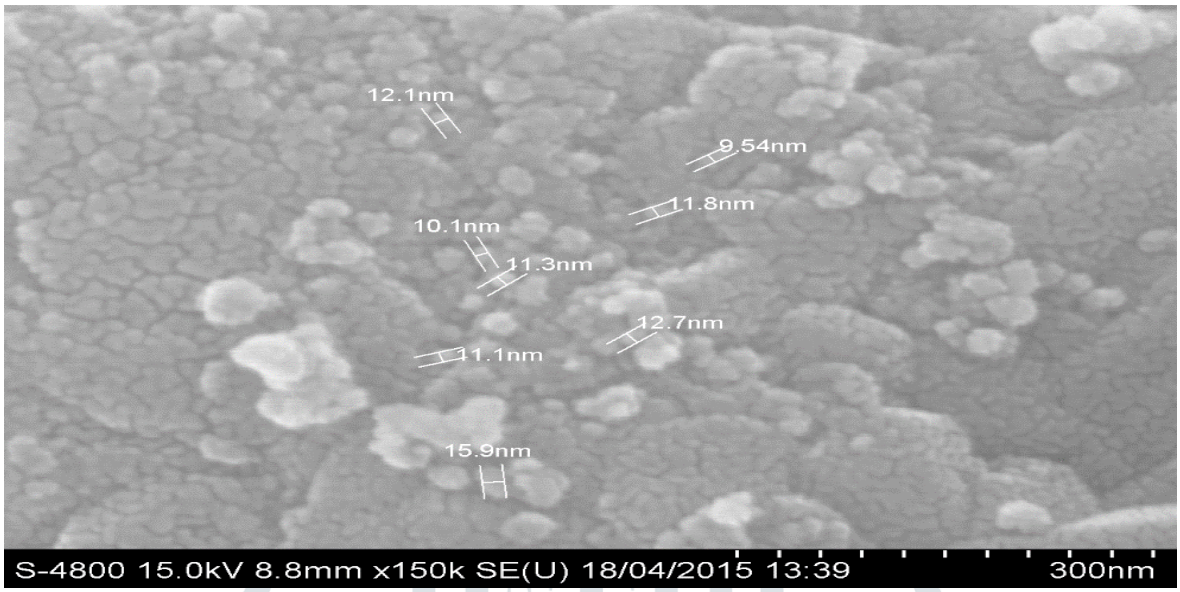

Fig. 3SEM image of $Sr_2Fe_{1-x}Ti_xMn_{0.2}NiO_6$ DP nanocomposites.

Fig. 3shows the structural morphology of the $Sr_2Fe_{1-x}Ti_xMn_{0.2}NiO_6$nanocomposites, which was investigated through FE-SEM. FE-SEM picture shows that the $Sr_2Fe_{1-x}Ti_xMn_{0.2}NiO_6$(x = 0.4) nanocomposites prepared by sol–gel method isuniform with some agglomeration of the nanoparticles were observed. The size of the particles, determined from the FE-SEM micrograph is in the order of 11–12 nm. These values of particle size are in good acceptance with the particle size calculated by Scherrer's formula.

3.1.3 Energy Dispersive X-ray (EDAX) Spectroscopy Analysis

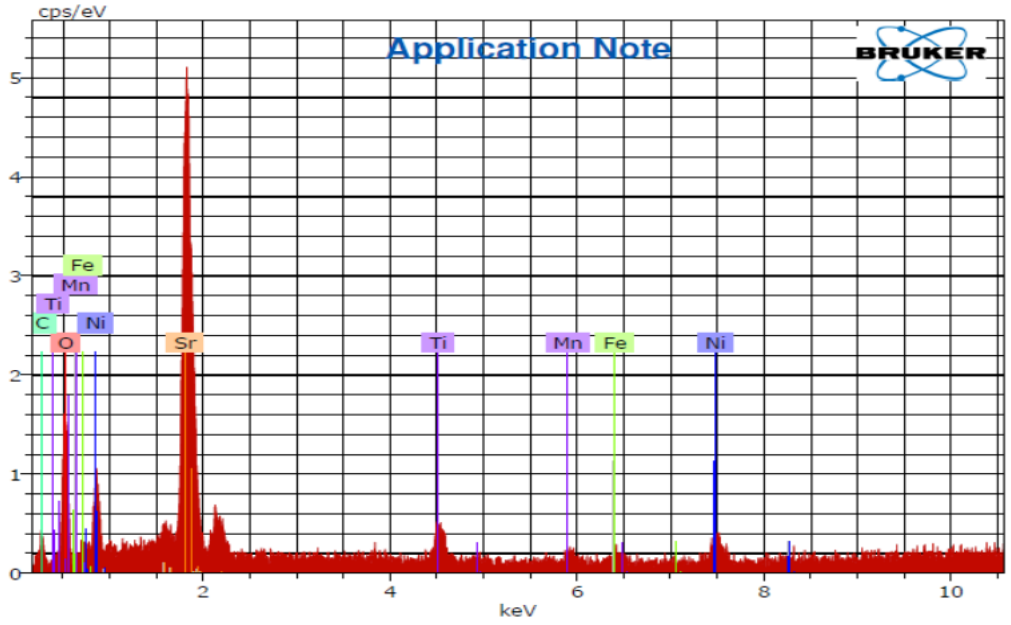

Fig. 4 EDAX pattern of $Sr_2Fe_{1-x}Ti_xMn_{0.2}NiO_6$nanocomposites.

EDAX analysis was done in order to determine the chemical composition on the surface of the sample to support our observations on the structure of Double Perovskite. From Fig. 4.Atomic weight percentages of various cations in the investigated samples are found to be approximately correct, which corresponds to a composition ratio and these ratios are expected by the preparation method.

3.2. Electrical conductivity

3.2.1. Impedance spectroscopy

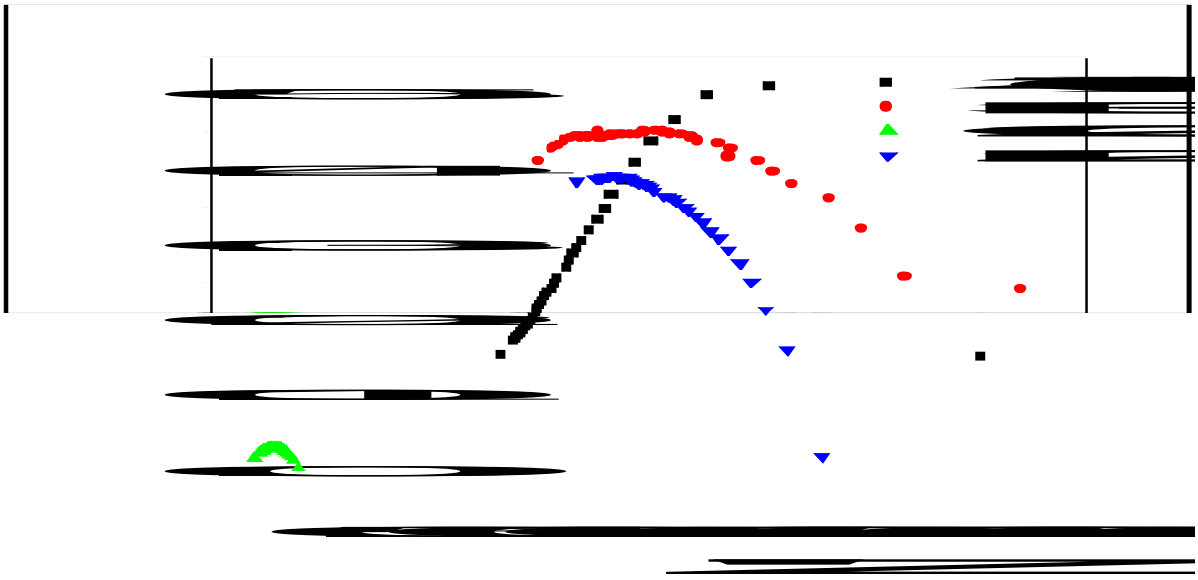

Fig. 5 Complex impedance spectra of the nanocrystalline$Sr_2Fe_{1-x}Ti_xMn_{0.2}NiO_6$of different concentrations.

The negative of imaginary part of impedance versus the real part of impedance plotted over a wide frequency range and at different temperatures are shown in fig. 5.The plot can give two semi-circles depending upon the electrical properties of the material. The first semicircle in the low frequency region represents the resistance of the grain boundary. The second one obtained for the high frequency domain correspondence to the resistance of grain or bulk properties [16,17]. It shows that only one semicircular arc has been obtained at low as well as at high temperatures and the diameter of semicircular arc becomes smaller with increasing temperature, referring to pronounced increase in dc conduction. It shows the predominating influence of the grain boundary impedance over the entire temperature range.The values of grain boundary resistance were found to decreases with increase in Ti content in $Sr_2Fe_{1-x}Ti_xMn_{0.2}NiO_6$nanocompsites. This decrease in resistance promotes electron hopping, which is known to be a mechanism for both conduction and polarization in double pervoskite.

3.2.2. Ac conductivity

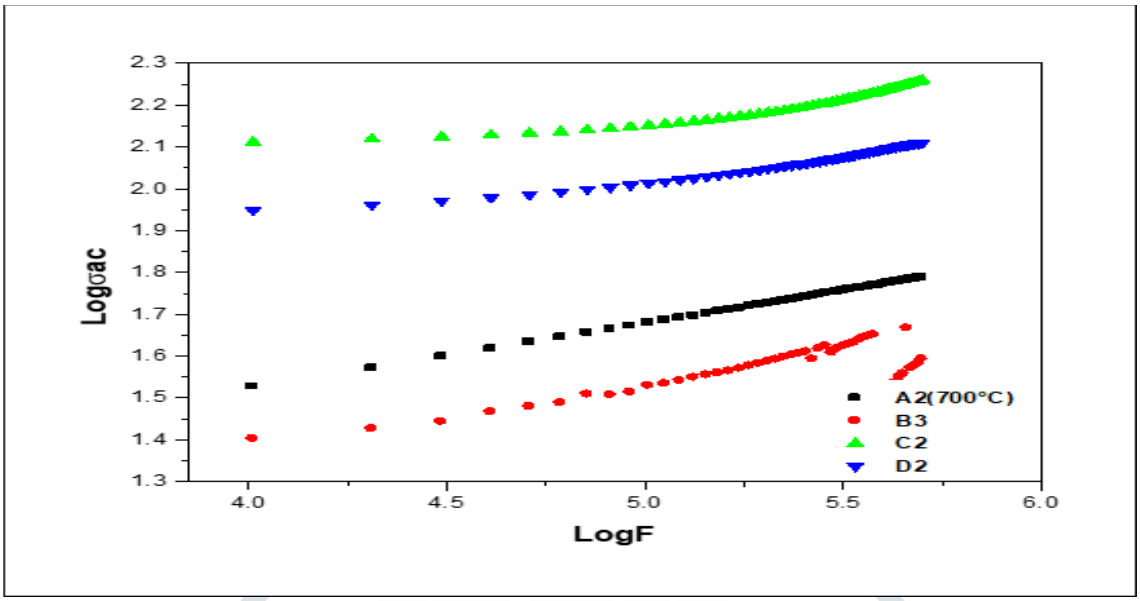

Fig. 6 Variation of ac conductivity with frequency at 700^0C of $Sr_2Fe_{1-x}Ti_xMn_{0.2}NiO_6$.

The ac conductivity(σ_{ac}) as a function of frequency at different temperatures was shown in fig. 6. It is evident that the plot of log σ_{ac}against log F gives straight lines with different slopes at high frequency range. The conductivity increases with increasing frequency and temperature.The ac conductivity was observed to increase slowly in the low frequency range. It increases rapidly in the high frequency region and becomes more and more frequency dependent. The dispersion of frequency dependent ac conductivity can be also described with the help of Koop's theory which supposed that dielectric medium behaves as multilayer capacitor consists of grains and grain boundaries. The behavior of grains and grain boundaries in the conduction mechanism changes with frequency [18]. At higher frequencies, the conduction is due to the grains only, which are less resistive as compared to grains boundaries. Therefore, ac conductivity increased sharply at higher frequencies due to the increase in electron hopping mechanism. Consequently, the increase in frequency enhances the hopping frequency of charge carriers resulting in an increase in the conduction process thereby increasing the ac conductivity. The value of ac conductivity has also been found to increase with Ti ion doping in $Sr_2Fe_{1-x}Ti_xMn_{0.2}NiO_6$ nanocompsites which is highest at (x = 0.4). It may be attributed to the various contributions to the polarization.

4. Conclusions

The Ti doping doubled pervoskite $Sr_2Fe_{1-x}Ti_xMn_{0.2}NiO_6$nanocomposite were synthesized by using sol-gel citrate method. XRD studies indicate that Sr_2FeNiO_6 have tetragonal structure and average crystallite size was nearly found to be ~18.11 nm. The Ti doped nanocomposites are uniform with some agglomeration of the nanoparticles were observed. The content of the metals in the double pervoskite nanocomposites are close to the theoretical values as shown by EDAX measurements.Impedance measurements reveal that the impedance response is dominated by grain boundary decrease with Ti doping up to x = 0.4 in $Sr_2Fe_{1-x}Ti_xMn_{0.2}NiO_6$ nanocomposite. The experimental results indicate that ac conductivity increases with Ti ion doping in $Sr_2Fe_{1-x}Ti_xMn_{0.2}NiO_6$ nanocompsites at x = 0.4 with constant temperature.

Reference

[1] Zaraq, A.; Orayech, B.; Faik, A.; Igartua, J.; Jouanneaux, A.; El Bouari, A. High temperature induced phase transitions in SrCaCoTeO6 and SrCaNiTeO6 ordered double perovskites. Polyhedron 2016, 110, 119–124.

[2] L. Xu, Y. Wan, H. Xie, Y. Huang, L. Yang, L. Qin, H. J. Seo, Synthesis, surface structure and optical properties of double perovskite Sr_2NiMoO_6 nanoparticles, Applied Surface Science; 2017, 169-4332 (16) 31553-7.

[3] D. Marrero-Lopez, J. Pena-Martinez, J.C. Ruiz-Morales, M. Gabas, P. Nunez, M.A.G. Aranda, J.R. Ramos-Barrado, Redox behavior, chemical compatibility and electrochemical performance of Sr_2MgMoO_6-δ as SOFC anode, Solid. State Ion. 180 (2010) 1672-1682.

[4] M. Pichler, D. Pergolesi, S. Landsmann, V. Chawla, J. Michler, M. Döbeli, A. Wokaun, T. Lippert, TiN-buffered substrates for photoelectrochemical measurements of oxynitride thin films, Appl. Surf. Sci. 369 (2016) 67-75

[5] J. Wang, C. Huang, X. Chen, H. Zhang, Z. Li, Z. Zou, Photocatalytic CO_2 reduction of $BaCeO_3$ with 4f configuration electrons, Appl. Surf. Sci. 358, (2015) 463-467

[6] S. Yang, D. Xu, B. Chen, B. Luo, X. Yan, L. Xiao, W. Shi, Synthesis and visible-light-driven photocatalytic activity of p-n heterojunction $Ag_2O/NaTaO_3$nanocubes, Appl. Surf. Sci. 383, (2016) 214-221

[7] S. Zhao, L.G. Gao, C.F. Lan, S.S. Pandey, S.Z. Hayase, T.L. Ma; First principles analysis of oxygen vacancy formation and migration in Sr2BMoO6 (B = Mg, Co, Ni), RSC Adv. 6 (2016) 31968-31975.

[8] X. Li, J. Yu, J. Low, Y. Fang, J. Xiaoc, X. Chen; Engineering heterogeneous semiconductors for solar water splitting. J. Mater. Chem. A, 3 (2015) 2485-2534

[9] E. Grabowska; Selected perovskite oxides: Characterization, preparation and photocatalytic properties-A review, Applied Catalysis B: Environmental, 186 (2016) 97-126

[10] M. A. Haddouch, A. Abbassi, Y. Aharbil, H. Labrim, Y. Tamraoui, F. Mirinioui, A. Benyoussef, L. Laanab, S. Benmokhtar; Journal of Applied Surfaces and Interfaces 1 (1-3) (2017) 1-6

[11] K.I.Kobayashi, T. Kimura, H. Sawada, K. Terakura, Y. Tokura; Nature 395 (1998) 677-680.

[12] R. J. Cava, B. Batlogg, J. J. Krajewski, R. Farrow, L.W. Rupp, A.E. White, K. Short, W.F. Peck, T. Kometani; Nature 332 (1988) 814 - 816.

[13]J. B. Goodenough, J. M. Longo; Physics.: Magnetic and Other Properties of Oxides and Related Compounds, Part a, Springer, Berlin, 4, (1970) 126-367.

[14] D. Marrero-López, J. Peña-Martínez, J.C. Ruiz-Morales, M. Gabás, P. Núñez, M.A.G. Aranda, J.R. Ramos-Barrado, Redox behavior, chemical compatibility and electrochemical performance of Sr2MgMoO6-δ as SOFC anode, Solid. State Ion. 180 (2010) 1672-1682.

[15] A.K. Dorai, Y. Masuda, J. Joo, S. Woo, S. Kim, Influence of Fe doping on the electrical properties of Sr2MgMoO6−δ. Mater. Chem. Phys. 139 (2013) 360-363.

[16] M. Hashim, S. Alimuddin, S. E. Kumar et al. Synthesis and characterizations of Ni2+ substituted cobalt ferrite nanoparticles. Mater Chem Phys. 139 (2013) 364–374.

[17] M. Hashim, S. Alimuddin, S. E. Kumar et al. Influence of Cr3+ ion on the structural, ac conductivity and magnetic properties of nanocrystalline Ni-Mg ferrite. Ceram Int. 139 (2013)1807–1819.

[18] M. Kamran , A. Ullah, S. Rahman et al. Structural, magnetic, and dielectric properties of multiferroic Co1-xMgxCr2O4 nanoparticles. J MagnMagn Mater.433 (2017) 178–186.